

Accepted Manuscript

Title: 1:1 and 2:1 Cocrystallizations of Alkoxy-Substituted Naphthalene Derivatives with Octafluoronaphthalene through Arene-Perfluoroarene Interactions

Author: Akiko Hori Haruhi Takeda J. Richard Premkumar G. Narahari Sastry



PII: S0022-1139(14)00289-9
DOI: <http://dx.doi.org/doi:10.1016/j.jfluchem.2014.09.025>
Reference: FLUOR 8442

To appear in: *FLUOR*

Received date: 3-7-2014
Revised date: 10-9-2014
Accepted date: 22-9-2014

Please cite this article as: A. Hori, H. Takeda, J.R. Premkumar, G.N. Sastry, 1:1 and 2:1 Cocrystallizations of Alkoxy-Substituted Naphthalene Derivatives with Octafluoronaphthalene through Arene-Perfluoroarene Interactions, *Journal of Fluorine Chemistry* (2014), <http://dx.doi.org/10.1016/j.jfluchem.2014.09.025>

This is a PDF file of an unedited manuscript that has been accepted for publication. As a service to our customers we are providing this early version of the manuscript. The manuscript will undergo copyediting, typesetting, and review of the resulting proof before it is published in its final form. Please note that during the production process errors may be discovered which could affect the content, and all legal disclaimers that apply to the journal pertain.

1:1 and 2:1 Cocrystallizations of Alkoxy-Substituted Naphthalene Derivatives with Octafluoronaphthalene through Arene-Perfluoroarene Interactions

Akiko Hori^a, Haruhi Takeda^a, J. Richard Premkumar^b, and G. Narahari Sastry^b

^a Department of Chemistry, School of Science, Kitasato University, Kitasato 1-15-1, Minami-ku, Sagami-hara, Kanagawa 252-0373

^b CSIR-Indian Institute of Chemical Technology, Centre for Molecular Modelling, Hyderabad-500607, India.

E-mail: hori@kitasato-u.ac.jp

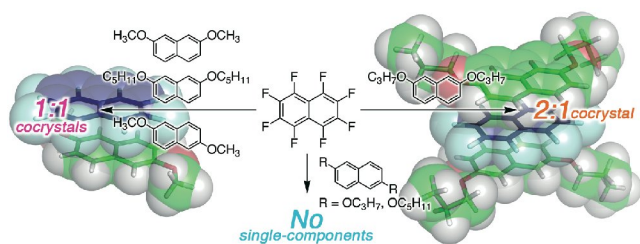
HIGHLIGHTS

- Alkoxy substituted naphthalenes were cocrystallized with octafluoronaphthalene.
- Arene-perfluoroarene interaction is observed in the cocrystals.
- The 2:1 cocrystal is rare example and each π -plane was highly overlapped.
- Alkoxy groups at 2,7-position in naphthalene are effective for the cocrystallization.
- Propoxy group is optimal to have possible CH \cdots F interactions to give cocrystals.

ABSTRACT

Naphthalene derivatives with laterally orientated short side chains readily form cocrystals with octafluoronaphthalene in which the position and the length of the lateral chain can control the 1:1 and 2:1 cocrystallization stoichiometries and overlapped areas of the π -planes, showing that the systematic substitution patterns in the chains of molecules can be exploited to rationally designed cocrystals.

Graphical Abstract



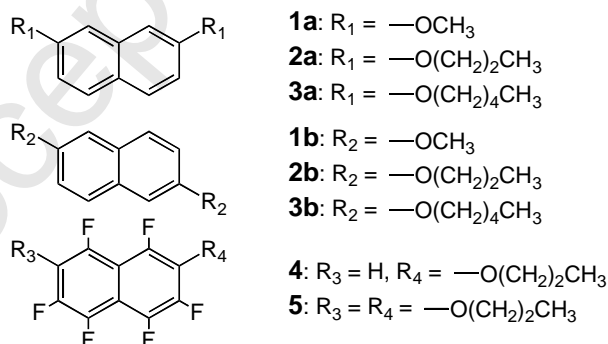
Naphthalene derivatives with laterally orientated short side chains readily form unique 1:1 and 1:2 cocrystals with octafluoronaphthalene through arene-perfluoroarene interactions.

1. Introduction.

The control of weak bonds and interactions has developed several important fields of supramolecular chemistry and crystal engineering in the last three decades [1,2]. Especially, the control of the π -interaction is an important subject for chemistry and biology, because the π -interactions behave as key interactions of molecular recognition events, self-assembly, and conductive properties [1-4]. The precise control of the position and direction of π -conjugated molecules is still challenging, because a rectangular orientation and a sliding orientation of the $\pi \cdots \pi$ interactions are predominantly formed [5-8], and the gas-phase study of benzene clusters showed that there is a competition between $\text{CH} \cdots \pi$ and $\pi \cdots \pi$ interactions [9a]. It also has been reported that in presence of metal ion the strength of $\text{CH} \cdots \pi$ interaction will reduce and $\pi \cdots \pi$ interaction will be enhanced for benzene dimer [9b]. However if the size of aromatic molecule increases, the stacking interaction will be more preferred than $\text{CH} \cdots \pi$ interactions [10]. Thus, we have attempted to make cocrystals through the arene-perfluoroarene interaction [3,11-15] in order to control the arrangements of the aromatic compounds, and several fluorinated molecules have been synthesized to create metal \cdots metal [16] and metal $\cdots \pi$ [17] supramolecular associations through these interactions.

In several cases, the arene-perfluoroarene interaction is an effective and powerful tool for the formation of unique cocrystals [11-16], but, unfortunately, the interaction has several limitations; *e.g.*, two or more substitutions of the laterally orientated side chains in an aromatic moiety decrease the strength of the interaction and flexible side chains hinder the cocrystallization. Thus, we

examined the cocrystallization of flexible alkoxy-chain substituted naphthalene derivatives, which increase the melting points and the strength of the arene-perfluoroarene interaction for comparison with the corresponding benzene derivatives. The target compounds are dimethoxy (**1**), dipropoxy (**2**), and dipentoxo (**3**) substituted naphthalenes, and the corresponding fluorinated naphthalenes **4-5**, as shown in Scheme 1. We successfully obtained new four cocrystals between alkoxy substituted naphthalene and octafluoronaphthalene ($C_{10}F_8$), while the alkoxy side chains on the naphthalene derivatives would produce steric repulsions in the crystal states. Furthermore, we discovered a 2:1 molecular ratio of the cocrystal of naphthalene derivative **2a** and $C_{10}F_8$, which is quite rare example, and two π -planes of **2a** and $C_{10}F_8$ are highly overlapped, compared with the cocrystal of the non-substituted naphthalene, $C_{10}H_8$, with $C_{10}F_8$ [18]. The results show that the systematic substitution patterns in the lateral chains of the naphthalene derivatives can control the cocrystallization behaviors; cocrystals were obtained between the alkoxynaphthalenes (**1a-3a** and **1b**) and $C_{10}F_8$ through arene-perfluoroarene interactions, while no cocrystals were obtained using **2b** and **3b**. Especially, the detailed structures of the 1:1 cocrystal of **1a**• $C_{10}F_8$, 2:1 cocrystal of (**2a**)₂• $C_{10}F_8$, and 1:1 cocrystal of **3a**• $C_{10}F_8$ will be discussed along with those of the single-component crystals **1a-3a** by using the crystallographic and computational studies.



Scheme 1.

2. Experimental

2.1. General.

All the chemicals were of reagent grade and used without further purification. Compounds **1-**

5 were prepared as previously reported, using the corresponding dihydroxy naphthalene and bromoalkane with K_2CO_3 [19]. 1H NMR spectral data were recorded on a Bruker AVANCEIII-400 spectrometer. Infrared spectra were recorded on a Shimadzu IR 8400s in KBr disk. The results of elemental analysis of C and H were collected by PerkinElmer PE2400 analyzer.

2.2. Preparations and characterization of cocrystals.

EtOH solutions of alkoxy naphthalene and $C_{10}F_8$ were combined to form the cocrystals. Typically, **1-3** (10 mmol) dissolved in EtOH (5 mL) and $C_{10}F_8$ (10 mmol) dissolved in EtOH (5 mL) were combined at room temperature to produce colorless needle microcrystals to give cocrystals, **1a**• $C_{10}F_8$, (**2a**)₂• $C_{10}F_8$, **3a**• $C_{10}F_8$, **1b**• $C_{10}F_8$, and single-components, **2b** and **3b**, respectively. They were clearly characterized by single crystal X-ray crystallographic studies. The results of elemental analysis show that $C_{10}F_8$ slowly removed by sublimation from the cocrystals at room temperature.

1a• $C_{10}F_8$. mp 90 °C dec. (the crystals slightly decomposed at 90 °C, and then new colorless prismatic crystals grew on the crystal surface, and the whole crystals melted at 135-138 °C). IR (KBr disk, cm^{-1}): 3431, 3013, 2971, 2943, 1663, 1628, 1516, 1479, 1404, 1389, 1211, 1119, 1034, 945, 841, 775. Elemental analysis: Calcd for $C_{22}H_{12}F_8O_2$ (%): C 57.40, H 2.63; found: C 56.99, H 2.49.

(**2a**)₂• $C_{10}F_8$. mp 77-78 °C (A part of the crystals melted at 77-78 °C and the whole crystals melted at 88-89 °C). IR (KBr disk, cm^{-1}): 2969, 2940, 2880, 1661, 1626, 1607, 1514, 1479, 1458, 1404, 1213, 945, 858, 835.

3a• $C_{10}F_8$. mp 51-52 °C (A part of the crystals melted at 51-52 °C and the whole crystals melted at 62-63 °C). IR (KBr disk, cm^{-1}): 2959, 2945, 2872, 1661, 1626, 1518, 1479, 1406, 1389, 1258, 1213, 1198, 1121, 1022, 945, 835, 785.

1b• $C_{10}F_8$. mp 110 °C dec. (the crystals slightly decomposed at 110 °C, and then new colorless prismatic crystals grew on the crystal surface, and the whole crystals melted at 133-156 °C). IR (KBr disk, cm^{-1}): 3021, 2969, 2945, 2843, 1663, 1605, 1506, 1478, 1466, 1402, 1234, 1206, 1159, 1117, 1032, 943, 856, 785, 590. Elemental analysis: Calcd for $C_{22}H_{12}F_8O_2$ (%): C 57.40, H 2.63; found: C 57.13, H 2.52.

2.3. X-ray crystallographic studies.

Single crystal X-ray structures were determined on a Bruker SMART APEX CCD diffractometer with graphite monochromator MoK α ($\lambda = 0.71073$ Å) generated at 50 kV and 35 mA. All crystals were coated by paratone-N and were measured at 100–233 K. For all compounds, cell refinement and reduction were performed by Bruker SAINT program, the structure solution was SHELXS97, the refinement was SHELXL97 [20]. Empirical absorption corrections were applied using the SADABS program [21]. All non-hydrogen atoms were refined anisotropically unless otherwise stated and hydrogen atoms were constrained at idealized positions, with the C–H distances of 0.95–0.99 Å. These data can be obtained free of charge from The Cambridge Crystallographic Data Center via www.ccdc.cam.ac.uk/data_request/cif.

1a•C₁₀F₈ (C₂₂H₁₂F₈O₂: $M_w = 460.32$): monoclinic, $P2_1$, $T = 233$ K, $a = 6.9034(4)$ Å, $b = 18.6158(10)$ Å, $c = 7.2620(4)$ Å, $\beta = 94.645(1)^\circ$, $V = 930.19(9)$ Å³, $Z = 2$, $D_c = 1.643$ g/cm³, $R_{\text{int}} = 0.0185$, No. reflns measured = 10505, No. independent = 4198, GOF = 1.043, $R((I) > 2\sigma(I)) = 0.0404$, $wR(F_o^2) = 0.1181$, CCDC 875019.

1b•C₁₀F₈ (C₂₂H₁₂F₈O₂: $M_w = 460.32$): triclinic, $P-1$, $T = 100$ K, $a = 6.829(3)$ Å, $b = 7.282(3)$ Å, $c = 9.671(4)$ Å, $\alpha = 68.235(3)^\circ$, $\beta = 84.193(4)^\circ$, $\gamma = 84.599(4)^\circ$, $V = 443.5(3)$ Å³, $Z = 1$, $D_c = 1.723$ g/cm³, $R_{\text{int}} = 0.0182$, No. reflns measured = 5067, No. independent = 1998, GOF = 1.044, $R((I) > 2\sigma(I)) = 0.0321$, $wR(F_o^2) = 0.0930$, CCDC 875022.

(2a)₂•C₁₀F₈ (C₄₂H₄₀F₈O₄: $M_w = 760.74$): monoclinic, $P2_1/c$, $T = 100$ K, $a = 13.014(3)$ Å, $b = 20.921(4)$ Å, $c = 6.8154(13)$ Å, $\beta = 103.496(2)^\circ$, $V = 1804.4(6)$ Å³, $Z = 2$, $D_c = 1.400$ g/cm³, $R_{\text{int}} = 0.0305$, No. reflns measured = 19819, No. independent = 4109, GOF = 1.151, $R((I) > 2\sigma(I)) = 0.0697$, $wR(F_o^2) = 0.2488$, CCDC 875020.

3a•C₁₀F₈ (C₃₀H₂₈F₈O₂: $M_w = 572.52$): triclinic, $P-1$, $T = 233$ K, $a = 6.9574(12)$ Å, $b = 14.683(3)$ Å, $c = 14.743(3)$ Å, $\alpha = 110.379(2)^\circ$, $\beta = 93.438(2)^\circ$, $\gamma = 101.820(2)^\circ$, $V = 1367.7(4)$ Å³, $Z = 2$, $D_c = 1.390$ g/cm³, $R_{\text{int}} = 0.0263$, No. reflns measured = 15288, No. independent = 6079, GOF =

1.129, $R(I) > 2\sigma(I) = 0.0779$, $wR(F_o^2) = 0.2496$, CCDC 875021.

3. Results and Discussion

3.1. Synthesis of cocrystals.

Compounds **1-3** were prepared using the corresponding dihydroxy naphthalene and bromoalkane with K_2CO_3 , based on previously reported procedures [19]. Single crystals **1-3** were prepared from EtOH (CCDC 875014-875018 are deposited), and no intermolecular $\pi \cdots \pi$ stacking was observed for the banana-shaped molecules of **1a-3a** and rod-shaped ones of **1b-3b**, because the intermolecular $CH \cdots \pi$ interactions between the alkoxy chains and naphthalene centers are dominant for all of the molecular packings, as shown in Fig. 1 (see Fig. S4 in Supporting Information). However, arrangements of the molecules are dramatically changed in the cocrystals in which the π - π stackings are clearly induced through the arene-perfluoroarene interactions, as shown below.

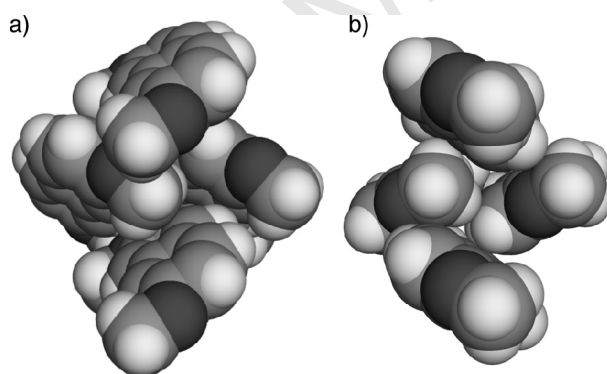


Fig. 1. Part of the crystal packing of (a) **1a** and (b) **1b**, showing the rectangular orientation of the molecular planes. Color scheme: C, gray; H, white; O, black.

Compound **1** and $C_{10}F_8$ were combined to form the cocrystals. Typically, two EtOH (5 mL) solutions of **1** (43 mg, 10 mmol) and $C_{10}F_8$ (58 mg, 10 mmol) were combined at room temperature, and the mixture was slowly concentrated to produce colorless prismatic crystals. The results of the GC-MS analysis of the first precipitated microcrystals indicated the formation of the 1:1 cocrystals, **1a**• $C_{10}F_8$ and **1b**• $C_{10}F_8$, in which two compounds exist in the same ratio in the microcrystals. The results of the elemental analysis also showed good agreements regarding the formation of the 1:1

cocrystals. Melting points of the cocrystals, **1a**•C₁₀F₈ (90 °C dec.) and **1b**•C₁₀F₈ (110 °C), were significantly lower than the single-component crystals, **1a** (138-139 °C) and **1b** (152-153 °C), which indicated the decomposition of the crystals by the elimination process of C₁₀F₈ (87 °C) [22]. The results indicate that the flexibility of the side chains influenced the crystal stability, while the arene-perfluoroarene interactions generally increase the melting points for cocrystallization [23]; the cocrystal C₁₀H₈•C₁₀F₈ was highly stabilized through arene-perfluoroarene interaction (mp 132 °C) to compare with the single components of C₁₀H₈ (80 °C) and C₁₀F₈ [18].

The structures and the packing formations of the cocrystals of **1a**•C₁₀F₈ and **1b**•C₁₀F₈ are shown in Fig. 2. In the crystal of **1a**•C₁₀F₈ (Fig. 2a) [24], **1a** and C₁₀F₈ are alternately aligned with face-to-face aromatic π -planes of the naphthalene moieties to form one dimer unit; the closest distance of the centroids of the naphthalene ‘ten’ atoms, C1-C2-C3-C4-C5-C6-C7-C8-C9-C10 (x, y, z) in **1a** and C13-C14-C15-C16-C17-C18-C19-C20-C21-C22 (x, y, z + 1) in C₁₀F₈, is 3.64 Å and the corresponding mean separation between the two planes (*i.e.*, the perpendicular distance from the ring centroid to the adjacent planes) is 3.33 Å, showing the remarkable π - π stacking. The distance between the corresponding two units, C1~C10 (x, y, z) in **1a** and C13~C22 (x, y, z) in C₁₀F₈, is 3.68 Å and the corresponding distance of the π - π stacking is 3.43 Å. On the other hand, **1b** and C₁₀F₈ in the cocrystal **1b**•C₁₀F₈ are alternately aligned with slightly twisted conformations because the π -planes of the naphthalene moieties overlap in a manner to avoid the side-chains (Fig. 2b). The distance of the centroids of the naphthalene atoms, C1-C2-C3-C4-C5-C1a-C2a-C3a-C4a-C5a in **1b** and C7b-C8b-C9b-C10b-C11b-C7c-C8c-C9c-C10c-C11c in C₁₀F₈, is 3.64 Å and the distance of the π - π stacking is 3.34 Å. In comparison, the distance of the non-substituted naphthalene and octafluoronaphthalene in the cocrystal (C₁₀H₈•C₁₀F₈) [18] is longer, 3.73 Å, and the corresponding distance of the π - π stacking is 3.42 Å, indicating that the methoxy groups not only hindered the supramolecular association through the arene-perfluoroarene interactions, but also closely arranged between the two π -plane’s centroids.

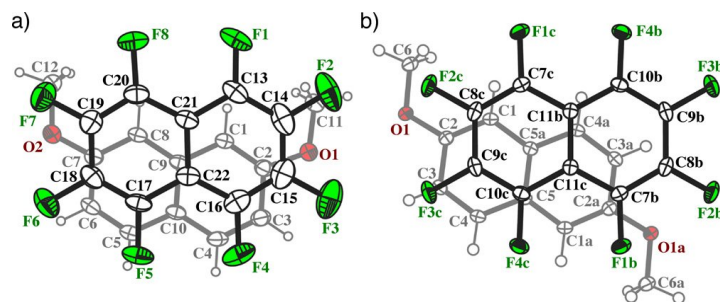


Fig. 2. The molecular structures of (a) **1a**•C₁₀F₈ and (b) **1b**•C₁₀F₈, showing the numbering schemes. Displacement ellipsoids are drawn at the 30 and 50% probability levels for **1a**•C₁₀F₈ (233K) and **1b**•C₁₀F₈ (100 K), respectively. Symmetry transformation used to generate equivalent atoms show a $(-x + 1, -y + 2, -z)$, b $(x, y + 1, z - 1)$, and c $(-x + 1, -y + 2, -z + 1)$.

In contrast, the results of the cocrystallization were monitored by GC-MS analysis. Crystals in a mixture of **2a-3a** and C₁₀F₈ show the cocrystallization, while only the single components of **2b-3b** are found in the crystals obtained from the mixtures of **2b-3b** and C₁₀F₈, for which the crystals are quickly collected during the early crystallization stage. These results indicate that not only the substitution numbers influence the cocrystallization behavior, but also the position of the alkoxy-chains trigger the molecular association through the arene-perfluoroarene interaction. It is pointed out that no cocrystallization of the propoxy-attached perfluoronaphthalene, **4** and **5**, was observed in the corresponding experiments. The melting points of (**2a**)₂•C₁₀F₈ (77-78 °C) and **3a**•C₁₀F₈ (51-52 °C) again show a slightly lower temperature than the single-component crystals, **2a** (81-82 °C) and **3a** (53-54 °C).

In (**2a**)₂•C₁₀F₈, octafluoronaphthalene is wrapped and sandwiched by two molecules of **2a** to give the 2:1 cocrystal (**2a**)₂•C₁₀F₈ in which the π -planes of the three naphthalene moieties are highly overlapped (Fig. 3). To the best of our knowledge, this is a rare example of a 2:1 cocrystal through an arene-perfluoroarene interaction, since the first example was reported by Marder *et al.* in 2004 [25,26]. A side-chain of each **2a** molecule partially wraps around the central molecule of C₁₀F₈ to give the trimer, (**2a**)₂•C₁₀F₈. The distance of the centroids of the naphthalene atoms, C1~C10 in **1a** and C17d-C18d-C19d-C20d-C21d-C17e-C18e-C19e-C20e-C21e in C₁₀F₈, is 3.57 Å and the

corresponding mean separation between the two planes is 3.31 Å. In the crystal packing, the three-molecule aggregates form a zig-zag arrangement (Fig. 4b).

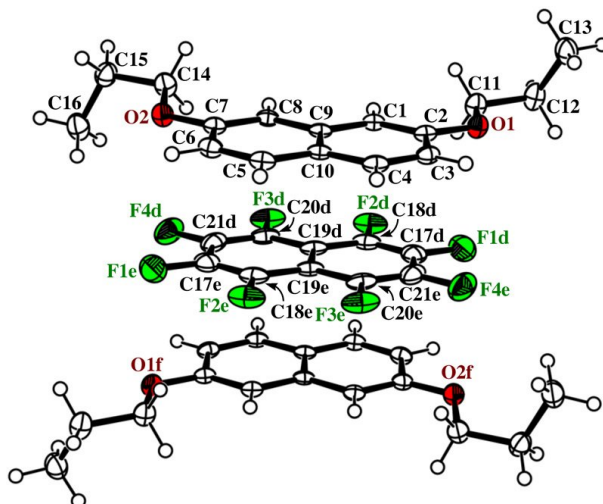


Fig. 3. ORTEP drawing of the crystal structure of $(2a)_2 \cdot C_{10}F_8$ at 100 K is shown with 50% probability thermal ellipsoids. Symmetry transformation used to generate equivalent atoms show d ($-x + 1, -y + 1, -z + 1$), e ($x - 1, y, z - 1$), and f ($-x, -y + 1, -z$).

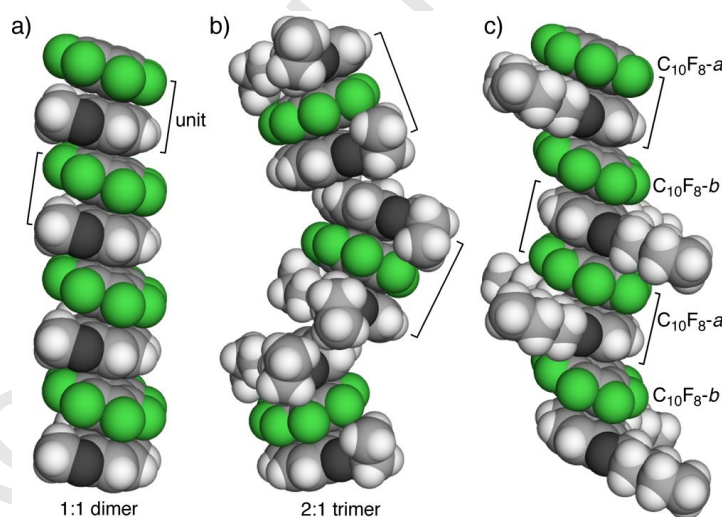


Fig. 4. Crystal packing of (a) $1a \cdot C_{10}F_8$, (b) $(2a)_2 \cdot C_{10}F_8$, and (c) $3a \cdot C_{10}F_8$ and the direction of stacking toward the c , b , and c axis, respectively.

In the cocrystal $3a \cdot C_{10}F_8$, **3a** and $C_{10}F_8$ are also alternately aligned with the face-to-face aromatic π -planes of the naphthalene moieties (Fig. 4c). The closest distance of the centroids of the naphthalene atoms, C1-C10 in **3a** and C21g-C25g-C21h-C25h (g: $x, y + 1, z$; h: $-x + 2, -y + 1, -z +$

1) in $C_{10}F_8$, is 3.66 Å and the corresponding mean separation between the two planes is 3.36 Å. The distance between C1-C10 (i) and C26c-C30c-C26i-C30i (i: $x + 1, y, z - 1$) is 3.75 Å and the distance to the adjacent planes is 3.39 Å. The directions of the pentoxy groups in **3a**• $C_{10}F_8$ and the methoxy groups of **1a**• $C_{10}F_8$ are alternately and regularly arranged, respectively, in each of the crystal packings.

3.2. Computational studies of cocrystals.

The experimental study showed that the arene-perfluoroarene mixture crystallizes in two different ratios (1:1 or 2:1). To understand this cocrystallization behavior, we have carried out the molecular modeling studies of the 1:1 and 2:1 stacked structures of the **1a** (methoxy), **2a** (propoxy), and **3a** (pentoxy) complexes of $C_{10}F_8$. The difference in the crystal formation ratio was found only in **2a**• $C_{10}F_8$ (2:1), while the other two mixtures crystallize in the 1:1 ratio. Therefore, we evaluated the crystal structures of the (**1a**)₂• $C_{10}F_8$, (**2a**)₂• $C_{10}F_8$, and (**3a**)₂• $C_{10}F_8$ and found a similarity in the **1a** and **3a** alkyl group arrangements of the $C_{10}F_8$ complexes, that is, the alkoxy carbons and the naphthalene ring are in a plane for **1a** and **3a** (Planar: **P**-conformation), but in **2a**, the methoxy groups exist up/down in the 2:1 cocrystal (Wrapped: **W**-conformation). Therefore, we modeled the **P**-conformations of the dimers (this only found in crystal structure), then the **P** and **W** conformations for the 2:1 trimers of **1a**, **2a**, and **3a** with $C_{10}F_8$ were examined. The optimization of the **W**-conformations of (**1a**)₂• $C_{10}F_8$ and (**3a**)₂• $C_{10}F_8$ collapsed into the corresponding **P**-conformations. For (**1a**)₂• $C_{10}F_8$ and (**3a**)₂• $C_{10}F_8$, the **P**-conformations are found to be energetically lower, and for (**2a**)₂• $C_{10}F_8$, as expected, the **W**-conformation is lower in energy than the **P**-conformation.

All the dimer and trimer energies were further improved by increasing the basis set from 6-31G* to cc-pVTZ, which are shown in the Supporting Information. The binding energies of the dimer and trimer can provide information about the trimerization energy. The binding energy can be calculated by evaluating the difference in the total energy of the complex and the individual monomers (in complexed state). In Table 1, we have listed the binding energy of the dimer (E_1) and trimer (E_2) at the M06-2X/cc-pVTZ level of theory. The binding energies of the dimer and trimer

increase as a function of the size of the alkyl chain, and as expected, the binding energy is found to be higher for the trimer than for the dimer. The difference in the binding energies of the trimer and dimer is called E_3 ($E_3 = E_1 - E_2$), and $E_1 - E_3$ is defined as the trimerization energy (E_4). To attain a trimer structure, the $(\mathbf{1a})_2 \cdot \text{C}_{10}\text{F}_8$ complex requires 1.34 kcal/mol energy so it prefers to be a dimer $\mathbf{1a} \cdot \text{C}_{10}\text{F}_8$ unit (1:1 ratio). The trimerization energy (E_4) clearly explains the experimentally observed 1:1 ratio for the $\mathbf{1a} \cdot \text{C}_{10}\text{F}_8$ complex. In contrast to the experiment, the $\mathbf{2a} \cdot \text{C}_{10}\text{F}_8$ complex prefers to be in a 1:1 ratio ($E_4 = 0.11$ kcal/mol) and the $\mathbf{3a} \cdot \text{C}_{10}\text{F}_8$ complex prefers to be in the 2:1 ratio ($E_4 = -0.27$ kcal/mol). For further understanding, we examined the relative energies of the **W** and **P**-conformations for $\mathbf{2a} \cdot \text{C}_{10}\text{F}_8$ and $\mathbf{3a} \cdot \text{C}_{10}\text{F}_8$. In the case of $\mathbf{3a} \cdot \text{C}_{10}\text{F}_8$, the **W**-conformation (partially wrapped structure, experimentally observed one for $(\mathbf{2a})_2 \cdot \text{C}_{10}\text{F}_8$) is 1.81 kcal/mol higher in energy than the **P**-conformation. The question that then arises, is the **W**-conformation make the crystallization as 2:1 ratio? If so, that type of conformation is higher in energy (not favorable) for the $\mathbf{3a} \cdot \text{C}_{10}\text{F}_8$ structure due to steric reasons and so it prefers the 1:1 form. The **P** and **W** conformations of $\mathbf{2a} \cdot \text{C}_{10}\text{F}_8$ are close in energy, however, the $\text{CH}_3 \cdots \text{F}$ interactions in $\mathbf{2a} \cdot \text{C}_{10}\text{F}_8$ make the **W**-conformation slightly lower in energy. The molecular electron density can be mapped through an ‘atoms in molecule’ procedure developed by Bader and coworkers [27]. To characterize the nature of the $\text{CH}_3 \cdots \text{F}$ interaction, we have calculated the electron density at the (3,-1) intermolecular bond critical point. The calculated intermolecular electron density at (3,-1) bond critical point (in between $\text{CH}_3 \cdots \text{F}$) is 0.004 a.u, considered to be a weak H-bond [28]. However, such a weak interaction is found not only between $\text{CH}_3 \cdots \text{F}$, but also between $\text{CH}_2 \cdots \text{F}$ as shown in Fig. 5. The recent computational study showed that $\text{CH} \cdots \text{M}$ interactions in metal-alkene complexes will increase strength of the non bonding interaction [29]. Interestingly, we found that the length of the propoxy group is optimal to have more possible $\text{CH} \cdots \text{F}$ interactions and this result explains the cocrystallization behavior of $\mathbf{2a}$ and C_{10}F_8 in the ratio of 2:1.

Table 1 The M06-2X/cc-pVTZ//M06-2X/6-31G* binding energy (kcal/mol) of the arene-perfluoroarene complexes.

R-group	dimer	trimer	$E_3 = E_2 - E_1$	Trimerization energy
	(E_1)	(E_2)		($E_4 = E_1 - E_3$)
1a	16.05	30.76	14.71	+1.34
2a	16.99	33.87	16.88	+0.11
3a	17.36	34.99	17.63	-0.27

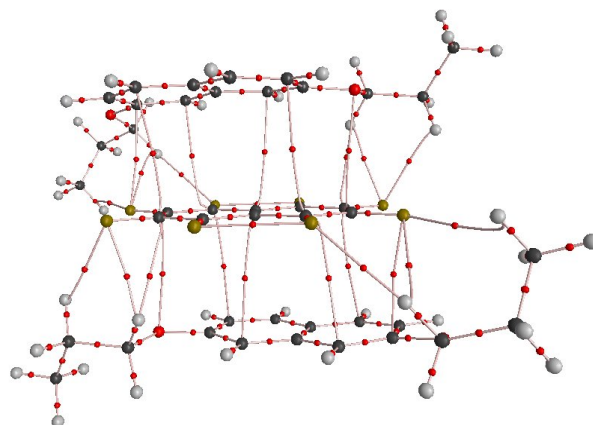


Fig. 5. The AIM molecular graph for $(2a)_2 \cdot C_{10}F_8$ in the W-conformation calculated at the M06-2X/6-31G* level of theory.

All the structures considered in this study were optimized at the M06-2X/6-31G* level of theory without any symmetry constraint. The binding energies of the dimer and trimers were calculated at the M06-2X/cc-pVTZ level on the M06-2X/6-31G* geometries. The geometry optimization and the binding energy calculations have been done using the Gaussian 09 program package [30]. To classify the strength of $CH_3 \cdots F$ interaction, we calculated the intermolecular (3,-1) bond critical point on M06-2X/6-31G* wave function files using the AIM2000 package [31]. All the optimized structure and principal geometries have been given in Supporting Information (Table S2 and Fig. S5-S11).

4. Conclusions

In conclusion, we found three types of cocrystals, 1:1 regular, 2:1 wrapped, and 1:1

alternately arranged structures, depending on the lengths of the attached alkoxy chains. The cocrystallization depends on the position of the flexible side chains, and the substitutions regulate the crystal packings. The length of the propoxy group seems to be the governing factor for the special arrangement between the alkoxyarene and perfluoroarene. The melting points of the cocrystals were clearly decreased with the increase of the side chain length; $C_{10}H_8 \cdot C_{10}F_8$ (132 °C) [18] > **1a**• $C_{10}F_8$ (90 °C dec.) > (**2a**)₂• $C_{10}F_8$ (77-78 °C) > and **3a**• $C_{10}F_8$ (51-52 °C), which indicates that the heat stability of the crystals decreases by longer flexible side chain. We correlated the distance between the two centroids of naphthalene derivatives with the side chain lengths and found an optical point at the propoxy group to give the 2:1 cocrystal; $C_{10}H_8 \cdot C_{10}F_8$ (3.73 Å), **1a**• $C_{10}F_8$ (3.68 Å), (**2a**)₂• $C_{10}F_8$ (3.57 Å), **3a**• $C_{10}F_8$ (3.66 Å). The remarkable short distance and highly overlapped structure of (**2a**)₂• $C_{10}F_8$ are formed by the W-conformation which was supported by the $CH_2 \cdots F$ and $CH_3 \cdots F$ weak interactions. Thus, suitable lengths of side chains stabilized the π - π interaction and formed unique cocrystals, which independently works of the thermodynamic stability of the crystal systems.

Acknowledgements. A.H thank Prof. Hidetaka Yuge and Mr. Yuuki Akimoto of Kitasato University for valuable discussion and helpful supports. G.N.S and J.R.P thank CSIR and DST, New Delhi for financial support.

References.

- [1] G.R. Desiraju (Ed.), Crystal Design. Structure and Function: Perspectives in Supramolecular Chemistry, Wiley, Chichester (2003) vol. 7.
- [2] (a) K. Reichenbacher, H.I. Süss, J. Hulliger, Chem. Soc. Rev. 34 (2005) 22-30; (b) B. Moulton, M.J. Zaworotko, Chem. Rev. 101 (2001) 1629-1658.
- [3] (a) E.A. Meyer, R.K. Castellano, F. Diederich, Angew. Chem. Int. Ed. 42 (2003) 1210-1250; (b) L.M. Salonen, M. Ellermann, F. Diederich, Angew. Chem. Int. Ed. 50 (2011) 4808-4842.
- [4] (a) M. Chourasia, G.M. Sastry, G.N. Sastry, Int. J. Biol. Macromol. 48 (2011) 540-552; (b) D. Umadevi, G.N. Sastry, J. Phys. Chem. Lett. 2 (2011) 1572-1576.

- [5] C. A. Hunter, J.K.M. Sanders, *J. Am. Chem. Soc.* 112 (1990) 5525-5534.
- [6] P. Hobza, H.L. Selzle, E.W. Schlag, *Chem. Rev.* 94 (1994) 1767-1785; K. Müller-Dethlefs, P. Hobza, *Chem. Rev.* 100 (2000) 143-167.
- [7] J.C. Ma, D.A. Dougherty, *Chem. Rev.* 97 (1997) 1303-1324.
- [8] M.O. Sinnokrot, C.D. Sherrill, *J. Phys. Chem. A* 110 (2006) 10656-10668.
- [9] (a) A.S. Mahadevi, A.P. Rahalkar, S.R. Gadre, G.N. Sastry, *J. Chem. Phys.* 133 (2010) 164308-1 to 164308-12; (b) D. Vijay, G.N. Sastry, *Chem. Phys. Lett.* 485 (2010) 235-242.
- [10] S. Grimme, *Angew. Chem. Int. Ed.* 47 (2008) 3430-3434.
- [11] A. Hori, *The importance of π -interactions in crystal engineering: frontiers in crystal engineering*, (Eds. E. R. Tiekink and J. Zukerman-Schpector), Wiley & Sons (2012) 163-185, and reference therein.
- [12] C.R. Patrick, G.S. Prosser, *Nature* 187 (1960) 1021.
- [13] J.H. Williams, *Acc. Chem. Res.* 26 (1993) 593-598.
- [14] (a) C. Dai, P. Nguyen, T.B. Marder, A.J. Scott, W. Clegg, C. Viney, *Chem. Commun.* (1999) 2493-2494; (b) T. M. Fasina, J.C. Collings, D.P. Lydon, D. Albesa-Jove, A.S. Batsanov, J.A.K. Howard, P. Nguyen, M. Bruce, A.J. Scott, W. Clegg, S.W. Watt, C. Viney and T.B. Marder, *J. Mater. Chem.* 14 (2004) 2395-2404.
- [15] (a) G.W. Coates, A.R. Dunn, L.M. Henling, D.A. Dougherty, R.H. Grubbs, *Angew. Chem. Int. Ed. Engl.* 36 (1997) 248-251; (b) A.F.M. Kilbinger, R.H. Grubbs, *Angew. Chem. Int. Ed.* 41, (2002) 1563-1566; (c) V.R. Vangala, A.Nangia, V.M. Lynch, *Chem. Commun.* (2002) 1304-1305.
- [16] A. Hori, A. Shinohe, M. Yamasaki, E. Nishibori, S. Aoyagi, M. Sakata, *Angew. Chem. Int. Ed.* 46 (2007) 7617-7620.
- [17] A. Hori, T. Arai, *CrystEngComm* 9 (2007) 215-217.
- [18] Crystal structure of $C_{10}H_8 \cdot C_{10}F_8$: J. Potenza, D. Mastropaolo, *Acta Cryst. B* 31 (1975) 2527-2529.
- [19] Z. Durmus, M. Biyiklioğlu, H. Kantekin, *Synthetic Metals* 159 (2009) 1563-1571.

- [20] G.M. Sheldrick, SHELXL-97. Program for crystal structure refinement, University of Göttingen, Germany (1997).
- [21] G.M. Sheldrick, SADABS. Empirical adsorption correction program for area detector data, University of Göttingen, Germany (1996).
- [22] The melting point of cocrystal through arene-perfluoroarene interaction fundamentally higher than the individual crystals. In these cases, melting points are found lower, which also examined by DSC.
- [23] The melting point of $C_6H_6 \cdot C_6F_6$ is 24 °C, which is much higher than the independent compounds (ref. 12).
- [24] The phase transition and decomposition of **1a**• $C_{10}F_8$ were started from 90°.
- [25] S.W. Watt, C. Dai, A.J. Scott, J.M. Burke, R.L.I. Thomas, J.C. Collings, C. Viney, W.Clegg, T. B. Marder, *Angew. Chem. Int. Ed.* 43 (2004) 3061–3063.
- [26] M. Kim, T.J. Taylor, F.P. Gabbaï, *J. Am. Chem. Soc.* 130 (2008) 6332-6333.
- [27] R.F.W.Bader, *Atoms in Molecules. A Quantum Theory*, Clarendon, Oxford, U. K (1990).
- [28] (a) R. Parthasarathi, V. Subramanian, N. Sathyamurthy, *J. Phys. Chem A* 110 (2006) 3349-3351; (b) S.J. Grabowski, W.A. Sokalski, E. Dyguda, J. Leszczynski, *J. Phys. Chem B* 110 (2006) 6444-6446.
- [29] J.R. Premkumar, D. Vijay, G.N. Sastry, *Dalton. Trans.* 41 (2012) 4965-4975.
- [30] M.J. Frisch, G.W. Trucks, H.B. Schlegel, G.E. Scuseria, M.A. Robb, J.R. Cheeseman, G. Scalmani, V. Barone, B. Mennucci, G.A. Petersson, H. Nakatsuji, M. Caricato, X. Li, H.P. Hratchian, A.F. Izmaylov, J. Bloino, G. Zheng, J.L. Sonnenberg, M. Hada, M. Ehara, K. Toyota, R. Fukuda, J. Hasegawa, M. Ishida, T. Nakajima, Y. Honda, O. Kitao, H. Nakai, T. Vreven, J.A. Montgomery, J.E. Peralta, F. Ogliaro, M. Bearpark, J.J. Heyd, E. Brothers, K.N. Kudin, V.N. Staroverov, R. Kobayashi, J. Normand, K. Raghavachari, A. Rendell, J.C. Burant, S.S. Iyengar, J. Tomasi, M. Cossi, N. Rega, N.J. Millam, M. Klene, J.E. Knox, J.B. Cross, V. Bakken, C. Adamo, J. Jaramillo, R. Gomperts, R.E. Stratmann, O. Yazyev, A.J. Austin, R. Cammi, C. Pomelli, J.W. Ochterski, R.L. Martin, K. Morokuma, V.G. Zakrzewski, G.S. Voth,

P. Salvador, J.J. Dannenberg, S. Dapprich, A.D. Daniels, O. Farkas, J.B. Foresman, J.V. Ortiz,

J. Cioslowski, D.J. Fox, Gaussian 09, Revision A.02, Gaussian, Inc., Wallingford, CT (2009).

[31] F. Biegler-Konig, J. Schonbohm, AIM2000, 2.0 (2002).

Accepted Manuscript